

## Bio-optical feedbacks among phytoplankton, upper ocean physics and sea-ice in a global model

Manfredi Manizza,<sup>1,2</sup> Corinne Le Quéré,<sup>1,3,4</sup> Andrew J. Watson,<sup>5</sup> and Erik T. Buitenhuis<sup>1</sup>

Received 18 June 2004; revised 10 September 2004; accepted 31 January 2005; published 3 March 2005.

[1] Phytoplankton biomass modifies the penetration of light and impacts the physical properties of the upper ocean. We quantify these impacts and the feedbacks on phytoplankton biomass for the global ocean using an Ocean General Circulation Model coupled to an ocean biogeochemistry model. Phytoplankton biomass amplifies the seasonal cycle of temperature, mixed layer depth and ice cover by roughly 10%. At mid and high latitudes, surface temperature warms by 0.1–1.5°C in spring/summer and cools by 0.1–0.3°C in fall/winter. In the tropics, phytoplankton biomass indirectly cools the ocean surface by 0.3°C due to enhanced upwelling. The mixed layer stratifies by 4–30 m everywhere except at high latitudes. At high latitudes, the sea-ice cover is reduced by up to 6% in summer and increased by 2% in winter, leading to further feedbacks on vertical mixing and heat fluxes. Physical changes drive a positive feedback increasing phytoplankton biomass by 4–12% and further amplifies the initial physical perturbations. **Citation:** Manizza, M., C. Le Quéré, A. J. Watson, and E. T. Buitenhuis (2005), Bio-optical feedbacks among phytoplankton, upper ocean physics and sea-ice in a global model, *Geophys. Res. Lett.*, 32, L05603, doi:10.1029/2004GL020778.

### 1. Introduction

[2] Marine phytoplankton can control Earth's temperature modulating the biogeochemical cycles of carbon and sulphur [Watson and Liss, 1998] but they can also absorb solar heat flux by pigments and modify upper ocean temperature [Morel, 1988]. Several studies have attempted to quantify this biophysical effect. Siegel *et al.* [1995] observed that in the equatorial Pacific Ocean phytoplankton blooms could increase the heating rate of the mixed layer by 0.13°C month<sup>-1</sup> and reduce the penetrative heat flux by -5.6 W m<sup>-2</sup> at 30 m. Strutton and Chavez [2004] observed a similar phenomenon during the El Niño/La Niña transition in the central equatorial Pacific Ocean in 1997/98. Sathyendranath *et al.* [1991] estimated a maximum biologically induced heating rate of 4°C month<sup>-1</sup> by using satellite data in the Arabian Sea. However, temperature changes in turn impact ocean dynamics.

[3] To estimate the response on ocean dynamics, this biophysical effect was incorporated into Ocean General Circulation Models (OGCM) using satellite-derived chlorophyll data as proxy of phytoplankton biomass. Nakamoto *et al.* [2000] showed that the presence of phytoplankton biomass not only warms the ocean surface but it also blocks the penetration of heat and cools the subsurface. The modification of the upper ocean thermal structure affected the currents in the equatorial oceans [Nakamoto *et al.*, 2001; Murtagudde *et al.*, 2002]. Shell *et al.* [2003], using the same kind of forcing, showed that this biophysical mechanism can affect the SST of the global ocean.

[4] Here we consider not only the impact of phytoplankton on ocean physics, but also the feedbacks on phytoplankton through the modified nutrient supply and light availability by using a global OGCM coupled to an ocean biogeochemistry model.

### 2. Modeling Strategy

[5] We use the OPA model, an OGCM based on primitive equations [Madec and Imbard, 1996; Madec *et al.*, 1999] which has an horizontal irregular grid with a resolution of about 2°. The latitudinal resolution is enhanced to ~0.5° at the equator and at high latitudes and the vertical resolution is 10 m in the top 100 meter. In OPA the vertical eddy diffusivity and viscosity coefficients are calculated by a 1.5 order turbulent kinetic energy model [Gaspar *et al.*, 1990]. Sub-grid eddy induced mixing is parameterized according to Gent and McWilliams [1990]. OPA is also coupled to LIM, a sea-ice model [Fichefet and Morales-Maqueda, 1999].

[6] We use three different model versions: (1) In the simulation labeled Dead Ocean (OPA<sub>DO</sub>), the penetration of solar radiation in the water column depends on the physical properties of seawater for mean open ocean condition and is computed by splitting the total surface irradiance  $I_o$  in two wavelength bands [Paulson and Simpson, 1977]:

$$I(z) = I_{IR} \cdot e^{-k_{IR}z} + I_{VIS} \cdot e^{-k_{VIS}z} \quad (1)$$

where the first and second right-hand terms represent the penetration of infrared and visible wavelength bands, respectively. The light attenuation coefficients  $k_{IR} = 2.86 \text{ m}^{-1}$  and  $k_{VIS} = 0.0434 \text{ m}^{-1}$  and the light partitioning ( $I_{IR} = I_o \cdot (0.58)$  and  $I_{VIS} = I_o \cdot (0.42)$ ) were estimated for mean open ocean conditions.  $z$  is depth.

[7] (2) In the simulation labeled SeaWiFS (OPA<sub>SW</sub>), we include the influence of phytoplankton on light penetration based on chlorophyll concentration ([Chl]) estimated from the SeaWiFS satellite (Figure 1 (top)). We also split the

<sup>1</sup>Max-Planck-Institut für Biogeochemie, Jena, Germany.

<sup>2</sup>Also at School of Environmental Sciences, University of East Anglia, Norwich, UK.

<sup>3</sup>Now at School of Environmental Sciences, University of East Anglia, Norwich, UK.

<sup>4</sup>Now also at British Antarctic Survey, Cambridge, UK.

<sup>5</sup>School of Environmental Sciences, University of East Anglia, Norwich, UK.

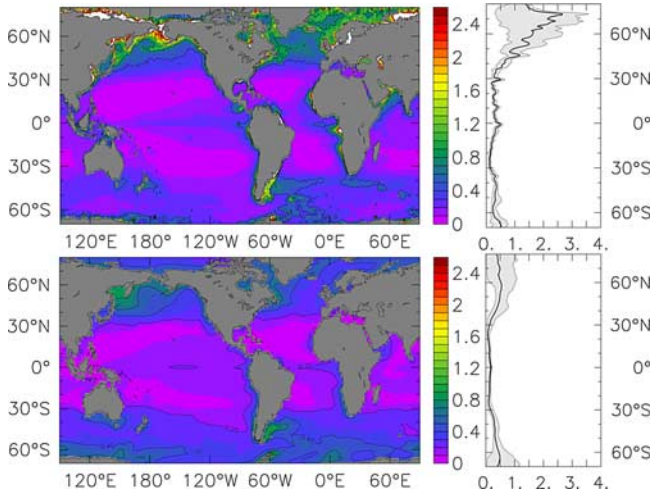


**Figure 1.** Surface chlorophyll concentration ( $\text{mg Chl m}^{-3}$ ) for (left) spatial distribution of annual average from (top) SeaWiFS and (bottom) DGOM and (right) zonal averaged for the annual mean (thick black line) and maximum and minimum monthly means (thin black lines) from (top) SeaWiFS and (bottom) DGOM. Grey area encompasses minimum and maximum monthly values. Contour interval is 0.2.

visible light in two averaged wavelength bands (red and blue/green):

$$I_{(z)} = I_{IR} \cdot e^{-k_{IR}z} + I_{RED} \cdot e^{-k_{(r)}z} + I_{BLUE} \cdot e^{-k_{(b)}z} \quad (2)$$

$$I_{RED} = I_{BLUE} = \frac{I_{VIS}}{2} \quad (3)$$

[8] We compute the light attenuation coefficient ( $k$ ), for the two bands as a function of chlorophyll concentration ([Chl]) [Morel, 1988]:

$$k_{(\lambda)} = k_{sw(\lambda)} + \chi_{(\lambda)} \cdot [\text{Chl}]^{e_{(\lambda)}} \quad (4)$$

The coefficients, derived from the visible light spectrum [Morel, 1988], are averaged in two bands [Foujols et al., 2000].  $\lambda$  is either red (r) or blue/green (b).  $k_{sw(\lambda)}$  is the light attenuation coefficient for optically pure seawater with values of 0.225 and 0.0232  $\text{m}^{-1}$  for red and blue/green respectively.  $\chi_{(\lambda)}$  is 0.037 and 0.074  $\text{m}^{-2} \text{mgChl m}^{-3}$  for the red and blue/green band, respectively and  $e_{(\lambda)}$  is 0.629 for red and 0.674 for the blue/green (no units).

[9] (3) In the simulation labeled Green Ocean ( $\text{OPA}_{GO}$ ), we consider the influence of phytoplankton on light penetration but in this case the [Chl] is computed by an ocean biogeochemistry model, the Dynamic Green Ocean Model (DGOM). In this third version, we also use the entire vertical profile of [Chl], taking into account the self shading effect caused by the presence of phytoplankton. The visible light is computed at every vertical level of the model ( $z$ ) as a function of the irradiance at the vertical level just above ( $z-1$ ), as follows:

$$I_{(z)} = I_{IR} \cdot e^{-k_{IR}z} + I_{RED(z-1)} \cdot e^{-k_{(r)}\Delta z} + I_{BLUE(z-1)} \cdot e^{-k_{(b)}\Delta z} \quad (5)$$

where  $\Delta z$  is the thickness of each layer between two vertical levels.

[10] The DGOM is a modified version of the PISCES model [Aumont et al., 2003]. It includes Phosphorous, Silicate, Iron and light co-limitation and represents five Plankton Functional Types (Nanophytoplankton, Diatoms and Coccolithophores for phytoplankton and meso and micro size classes for zooplankton) [Le Quéré et al., 2005]. In  $\text{OPA}_{GO}$  the total [Chl] is the sum of the chlorophyll of all three phytoplankton types.

[11] The DGOM reproduces the spatial gradients observed by SeaWiFS, although the model underestimates the surface [Chl] in the North Atlantic ( $>50^\circ\text{N}$ ). The model is initialized with observations both for the physics and the biogeochemistry. The model was forced by NCEP re-analyzed fields [Kalnay et al., 1996]. Simulations are run for 10 years. We present results for the year 2000.

### 3. Results and Discussion

[12] The differences between  $\text{OPA}_{SW}$  and  $\text{OPA}_{DO}$  show the impact of the presence of phytoplankton on the physical properties of the upper ocean, while the differences between  $\text{OPA}_{GO}$  and  $\text{OPA}_{DO}$  show all the feedbacks between the physical properties of the upper ocean and the presence of phytoplankton.

[13] The presence of phytoplankton induces an annual mean cooling of the SST ( $\Delta\text{SST}$ ) by  $0.3^\circ\text{C}$  in the tropics and a warming by  $0.05^\circ\text{C}$  in the sub-tropics (Figure 2a). The tropical cooling is caused by an enhanced upwelling in  $\text{OPA}_{GO}$ . Similar tropical cooling have been published by Nakamoto et al. [2001] but not reproduced by Murtugudde

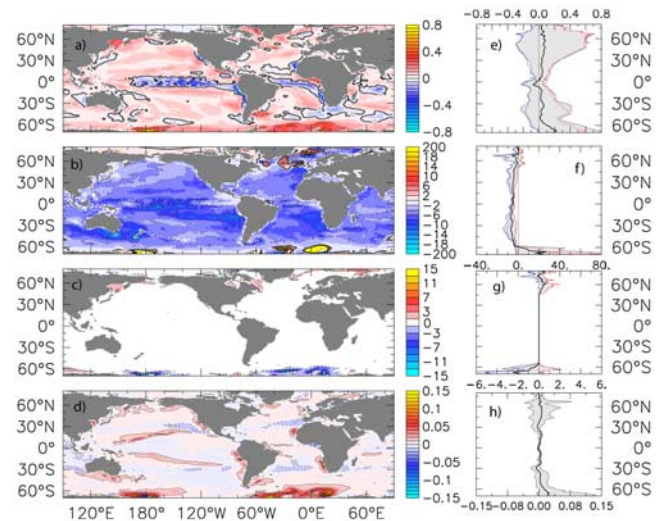


**Figure 2.** Annual mean of (a)  $\Delta\text{SST}$  ( $^\circ\text{C}$ ), (b)  $\Delta\text{MLD}$  (meter) and (c)  $\Delta\text{sea-ice cover}$  (%) and (d)  $\Delta[\text{Chl}]$  at surface ( $\text{mg Chl}^{-3}$ ) for  $\text{OPA}_{GO}$  minus  $\text{OPA}_{DO}$ . Zonal annual average for the (e)  $\Delta\text{SST}$ , (f)  $\Delta\text{MLD}$ , (g)  $\Delta\text{sea-ice cover}$  and (h)  $\Delta[\text{Chl}]$  at surface. Grey area encompasses maximum and minimum monthly values. Red and blue lines indicate respectively maximum and minimum values of difference for  $\text{OPA}_{SW}$  and  $\text{OPA}_{DO}$ . The contour interval is (a) 0.05, (b) 2, (c) 2, (d) 0.02.

*et al.* [2002]. We have performed additional simulations with a different bio-optical model which reproduced the same results at mid and high latitudes but led to tropical warming rather than cooling (results not shown). These contradicting results in the tropics suggest that the readjustment of the upwelling does not appear robust and is very sensitive to both the control simulations and the chosen parameters.

[14] The warming at mid and high latitudes is caused by the absorption of heat by phytoplankton. The monthly SST change mirrors the evolution of [Chl] over the year, with minimum values in winter and maximum values during the spring bloom (Figure 2e). The range of the zonal mean seasonal amplitude increases from the sub-tropics ( $-0.2^{\circ}\text{C}$  to  $+0.3^{\circ}\text{C}$ ) to the high latitudes ( $-0.3^{\circ}\text{C}$  to  $+0.6^{\circ}\text{C}$ ) (Figure 2e).

[15] Everywhere in the ocean the presence of phytoplankton induces cooling of the subsurface layers below ca 30 m because the incoming radiation is trapped at the surface (Data not shown here). In fall and winter, surface waters are mixed with cold sub-surface waters. This process produces a relative higher cooling of SST in  $\text{OPA}_{GO}$ .

[16] The change in the thermal structure also produces a change in the stratification of the upper ocean as shown by the difference in Mixed Layer Depth ( $\Delta\text{MLD}$ ) (Figure 2b). The presence of phytoplankton shoals the MLD by ca 5 m on global annual average. As with  $\Delta\text{SST}$ ,  $\Delta\text{MLD}$  show patterns which follow the seasonal variability of the algal biomass as a function of latitude. The seasonal amplitude of  $\Delta\text{MLD}$  increases from the tropics to high latitudes with maximum values at  $60^{\circ}$  in both hemispheres. The increase in stratification is maximum (by ca  $-20$  meter) during the spring bloom in both hemispheres.

[17] The presence of phytoplankton and associated warming produces a reduction in sea-ice cover by ca 2–6% in summer, in agreement with [Zeebe *et al.*, 1996]. The enhanced ice-free zones are susceptible to the winter atmospheric forcing which causes convection and a deeper winter mixed layer by 80 meter (Figure 2f). During winter, on the other hand, cooling enhances ice formation (Figures 3d and 3h).

[18] The difference between  $\text{OPA}_{GO}$  and  $\text{OPA}_{SW}$  highlights the impact of using modeled [Chl] rather than satellite data. The differences can be caused by three factors. First, the surface [Chl] are different. Second, only in  $\text{OPA}_{GO}$  do the phytoplankton respond to the modifications of the physical environment. Third,  $\text{OPA}_{GO}$  considers the self shading effect and uses the entire vertical profile of [Chl], whereas  $\text{OPA}_{SW}$  uses only the [Chl] at the surface.

[19] To test the importance of the self shading effect, we carried out a sensitivity analysis using surface [Chl] computed by the DGOM in the equation (2), as used in  $\text{OPA}_{SW}$ . The tropical cooling in the intermediate simulation is as large as in the  $\text{OPA}_{GO}$  simulation, which indicates that the self shading plays only a small role, and the differences between  $\text{OPA}_{GO}$  and  $\text{OPA}_{SW}$  are mostly caused by the different [Chl] in the tropics, even because in that specific region there is no significant change in [Chl] as result of a possible biophysical feedback. At high latitudes the self shading effect has a negligible impact whereas the feedbacks between ocean physics and phytoplankton, involving also sea-ice cover, play an important role.

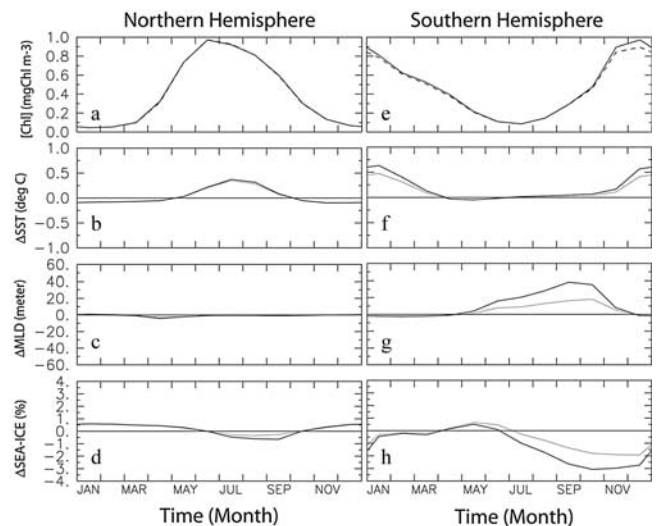


**Figure 3.** Seasonal cycle averaged between  $55^{\circ}$  and  $90^{\circ}$  for the northern (left) and southern (right) hemisphere for (a,e) surface [Chl] ( $\text{mg m}^{-3}$ ) (full line is  $\text{OPA}_{GO}$  and dashed line is  $\text{OPA}_{DO}$ ), (b,f)  $\Delta\text{SST}$  ( $^{\circ}\text{C}$ ), (c,g)  $\Delta\text{MLD}$  (meter), (d,h)  $\Delta\text{sea-ice cover}$  (%) between (full line)  $\text{OPA}_{GO}$  and  $\text{OPA}_{DO}$  and (dotted line)  $\text{OPA}_{SW}$  and  $\text{OPA}_{DO}$ . The difference between the full line and the dotted line in the panels (b–d) and (f–h) represents the feedbacks of phytoplankton in response to changes in physical properties of the surface waters.

[20] Maximum and minimum values of  $\Delta\text{SST}$  and  $\Delta\text{MLD}$  are similar at low latitudes in  $\text{OPA}_{GO}$  and  $\text{OPA}_{SW}$  (Figures 2e and 2f). The tropical cooling and ice melting are more pronounced when the biogeochemical model is used. In the tropics the different biological forcing applied (prognostic vs diagnostic) is responsible for the different modifications in the thermal structure and for the vertical circulation of the tropical zones.

[21] The sea-ice melting, due to the presence of phytoplankton (Figure 2g), is larger in  $\text{OPA}_{GO}$  than in  $\text{OPA}_{SW}$ , in spite of the fact that DGOM [Chl] is lower than that in SeaWiFS in the Northern hemisphere and about the same in the Southern hemisphere (Figure 1). In  $\text{OPA}_{SW}$  the chlorophyll data are used as passive forcing and they do not respond to the changes in the physical environment due to the presence of phytoplankton. However, in  $\text{OPA}_{GO}$  the modifications in the upper ocean structure created by the biological effect (i.e., less sea-ice cover) in turn increased the phytoplankton biomass (Figure 3e) and further produced a more substantial sea-ice melting effect (Figures 3d and 3h), especially in the Southern Ocean. Thus there is a positive feedback between phytoplankton dynamics, SST, sea-ice cover and solar radiation: during summer, phytoplankton blooms warm the SST which melts the sea-ice (Figures 3d and 3h). The sea-ice cover is thus reduced and in turn it allows the solar radiation to reach the surface and enhance phytoplankton growth.

[22] It is difficult to assess the importance of this biophysical feedback for the global ocean using our forced experiments. However the changes in ocean physics shown here are of the same order of magnitude (in percent) as the

changes in both carbon sink [Le Quéré et al., 2005] and dimethylsulphide emissions [Bopp et al., 2004] estimated under different climatic conditions.

#### 4. Conclusions

[23] Our results suggest that the presence of phytoplankton causes (1) SSTs warming by up to 0.8°C in spring (with local peaks of 1.5°C) and cooling by up to 0.3 in winter, (2) subsurface temperature cooling by 0.1°C to 1.1°C, (3) surface ocean stratification between 4 and 30 m all year except at high latitudes, and (4) summer sea-ice cover decrease by 0.5 to 6%. These effects feedback on phytoplankton biomass which increases by up to 12% depending on the region. Changes in SST and stratification are enhanced by 4 and 3%, respectively, when a biogeochemistry model is used due to the feedbacks between ocean physics and phytoplankton biomass.

[24] The results presented here suggest that phytoplankton have a consistent impact on the physical structure of the top part of the ocean and are affected by those changes in return. Whereas the extra-tropical SST warming and associated stratification appear robust, other results do not. The tropical cooling is sensitive to the choice of model parameters. This is also the case for the response of the marine ecosystems. Global marine ecosystem models are in their early stages of development. Our study shows that more research need to be carried out to understand this feedback, especially using coupled atmosphere-ocean models [Timmermann and Jin, 2002; Shell et al., 2003].

[25] Phytoplankton could have an additional impact on regulating the ocean carbon cycle not only by the direct uptake of CO<sub>2</sub> and its export towards deep ocean, but also by affecting its solubility, mixing rate and areas of sink through modifications of respectively SST, MLD and sea-ice cover. From this, we infer that the distinction between physical and biological oceanic carbon pump may not be as distinct as thought so far.

[26] The absorption of light by phytoplankton is also species and size dependent [Yentsch and Phinney, 1989], thus bio-optical parameterizations for each phytoplankton group need to be taken into account in future work.

[27] **Acknowledgments.** We thank N. Lefèvre and the Dynamic Green Ocean Project participants for their suggestions, K. Rodgers and the OPA team for support, the DKRZ for computer time and two anonymous reviewers for their comments. Plots were made using Ferret. MM was supported by both the LINKECOL fellowship from ESF and the NOCES project, contract EVK2-CT-2001-00134.

#### References

Aumont, O., E. Maier-Reimer, S. Blain, and P. Monfray (2003), An ecosystem model of the global ocean including Fe, Si, P colimitations, *Global Biogeochem. Cycles*, *17*(2), 1060, doi:10.1029/2001GB001745.  
 Bopp, L., O. Boucher, O. Aumont, S. Belviso, J.-L. Dufresne, M. Pham, and P. Monfray (2004), Will marine dimethylsulphide emissions amplify or

alleviate global warming? A model study, *Can. J. Fish. Aquat. Sci.*, *61*, 826–835.  
 Fichefet, T., and M. A. Morales-Maqueda (1999), Modelling the influence of snow accumulation and snow-ice formation on the seasonal cycle of the Antarctic sea-ice cover, *Clim. Dyn.*, *15*, 251–268.  
 Foujols, M., M. Lévy, O. Aumont, and G. Madec (2000), *OPA8.1 Tracer Model Reference Manual*, Inst. Pierre Simon Laplace, Paris.  
 Gaspar, P., Y. Gregoris, and J. M. Lefèvre (1990), A simple kinetic energy model for simulations of the oceanic vertical mixing: Tests at station Papa and Long-Term Upper Ocean Study Site, *J. Geophys. Res.*, *95*, 16,179–16,193.  
 Gent, P. R., and J. C. McWilliams (1990), Isopycnal mixing in the ocean circulation models, *J. Phys. Oceanogr.*, *20*, 150–155.  
 Kalnay, E., et al. (1996), The NCEP/NCAR 40-year reanalysis project, *Bull. Am. Meteorol. Soc.*, *77*, 437–471.  
 Le Quéré, C., et al. (2005), Ecosystem dynamics based on plankton functional types for global ocean biogeochemistry models, *Global Change Biol.*, in press.  
 Madec, G., and M. Imbard (1996), A global ocean mesh to overcome the north pole singularity, *Clim. Dyn.*, *12*, 381–388.  
 Madec, G., P. Delecluse, M. Imbard, and C. Lévy (1999), *OPA 8.1 Ocean General Circulation Model Reference Manual*, Lab. d'Océanogr. Dyn. et de Climatol., Paris.  
 Morel, A. (1988), Optical modelling of the upper ocean in relation to its biogenous matter content (case I waters), *J. Geophys. Res.*, *93*, 10,749–10,768.  
 Murtugudde, R., J. Beauchamp, C. R. McClain, M. Lewis, and A. J. Busalacchi (2002), Effects of penetrative radiation on the upper tropical ocean circulation, *J. Clim.*, *15*, 470–486.  
 Nakamoto, S., S. P. Kumar, J. M. Oberhuber, K. Muneyama, and R. Frouin (2000), Chlorophyll modulation of sea surface temperature in the Arabian Sea in a mixed-layer isopycnal general circulation model, *Geophys. Res. Lett.*, *27*, 747–750.  
 Nakamoto, S., S. P. Kumar, J. M. Oberhuber, J. Ishizaka, K. Muneyama, and R. Frouin (2001), Response of the equatorial Pacific to chlorophyll pigment in a mixed layer isopycnal ocean general circulation model, *Geophys. Res. Lett.*, *28*, 2021–2024.  
 Paulson, C. A., and J. J. Simpson (1977), Irradiance measurements in the upper ocean, *J. Phys. Oceanogr.*, *7*, 952–956.  
 Sathyendranath, S., A. D. Gouveia, A. R. Shetye, P. Ravindran, and T. Platt (1991), Biological control of surface temperature in the Arabian Sea, *Nature*, *349*, 54–56.  
 Shell, K. M., R. Frouin, S. Nakamoto, and R. C. J. Somerville (2003), Atmospheric response to solar radiation absorbed by phytoplankton, *J. Geophys. Res.*, *108*(D15), 4445, doi:10.1029/2003JD003440.  
 Siegel, D. A., J. C. Ohlmann, L. Washburn, R. Bidigare, C. T. Noss, E. Fields, and Y. Zhou (1995), Solar radiation, phytoplankton pigments and the radiant heating of the equatorial Pacific warm pool, *J. Geophys. Res.*, *100*, 4885–4891.  
 Strutton, P. G., and F. P. Chavez (2004), Biological heating in the equatorial Pacific: Observed variability and potential for real-time calculation, *J. Clim.*, *17*, 1097–1109.  
 Timmermann, A., and F. Jin (2002), Phytoplankton influences on tropical climate, *Geophys. Res. Lett.*, *29*(23), 2104, doi:10.1029/2002GL015434.  
 Watson, A. J., and P. S. Liss (1998), Marine biological controls on climate via the carbon and sulphur geochemical cycles, *Philos. Trans. R. Soc. London, Ser. B*, *353*, 41–51.  
 Yentsch, C. S., and D. A. Phinney (1989), A bridge between ocean optics and microbial ecology, *Limnol. Oceanogr.*, *34*, 1694–1705.  
 Zeebe, R. E., H. Eicken, D. H. Robinson, D. Wolf-Gladrow, and G. S. Dieckmann (1996), Modeling the heating and melting of sea ice through light absorption by microalgae, *J. Geophys. Res.*, *101*, 1163–1181.

E. T. Buitenhuis and M. Manizza, Max Planck Institut für Biogeochemie, Postfach 100164, D-07701 Jena, Germany. (mmanizza@bgc-jena.mpg.de)  
 C. Le Quéré and A. J. Watson, School of Environmental Sciences, University of East Anglia, Norwich NR4 7TJ, UK.